More on black holes perceiving the dark dimension

Luis A. Anchordoqui,[1,2,3] Ignatios Antoniadis,[4,5] and Dieter Lüst[6,7]
[1]*Department of Physics and Astronomy, Lehman College, City University of New York, Bronx, New York 10468, USA*
[2]*Department of Physics, Graduate Center, City University of New York, Manhattan, New York 10016, USA*
[3]*Department of Astrophysics, American Museum of Natural History, Manhattan, New York 10024, USA*
[4]*High Energy Physics Research Unit, Faculty of Science, Chulalongkorn University, Bangkok 1030, Thailand*
[5]*Laboratoire de Physique Théorique et Hautes Énergies - LPTHE, Sorbonne Université, CNRS, 4 Place Jussieu, 75005 Paris, France*
[6]*Max-Planck-Institut für Physik, Werner-Heisenberg-Institut, 80805 München, Germany*
[7]*Arnold Sommerfeld Center for Theoretical Physics, Ludwig-Maximilians-Universität München, 80333 München, Germany*

(Received 14 May 2024; accepted 29 May 2024; published 3 July 2024)

In the last two years, the dark dimension scenario has emerged as focal point of many research interests. In particular, it functions as a stepping stone to address the cosmological hierarchy problem and provides a colosseum for dark matter contenders. We reexamine the possibility that primordial black holes (PBHs) perceiving the dark dimension could constitute all of the dark matter in the Universe. We reassess limits on the abundance of PBHs as dark matter candidates from γ-ray emission resulting from Hawking evaporation. We reevaluate constraints from the diffuse γ-ray emission in the direction of the Galactic Center that offer the best and most solid upper limits on the dark matter fraction composed of PBHs. The revised mass range that allows PBHs to assemble all cosmological dark matter is estimated to be $10^{15} \lesssim M_{\rm BH}/{\rm g} \lesssim 10^{21}$. We demonstrate that, due to the constraints from γ-ray emission, quantum corrections due to the speculative memory burden effect do not modify this mass range. We also investigate the main characteristics of PBHs that are localized in the bulk. We show that PBHs localized in the bulk can make all cosmological dark matter if $10^{11} \lesssim M_{\rm BH}/{\rm g} \lesssim 10^{21}$. Finally, we comment on the black holes that could be produced if one advocates a space with two boundaries for the dark dimension.

DOI: 10.1103/PhysRevD.110.015004

I. INTRODUCTION

The swampland program seeks to distinguish effective theories that can be completed into quantum gravity in the ultraviolet from those that cannot [1]. In theory space, the swampland frontier is drawn by a family of conjectures classifying the properties that an effective field theory should have/avoid to enable a consistent completion into quantum gravity. These conjectures deliver a bridge from quantum gravity to astrophysics, cosmology, and particle physics [2–4].

For example, the distance conjecture (DC) asserts that along infinite distance geodesics there is an infinite tower of states that become exponentially light asymptotically [5]. Connected to the DC is the anti–de Sitter (AdS) distance conjecture [6], which ties in the dark energy density to the mass scale m characterizing the infinite tower of states, $m \sim |\Lambda|^{\alpha}$, in the limit of a small negative AdS vacuum energy with α a positive constant of $\mathcal{O}(1)$. In addition, under the hypothesis that this scaling behavior remains valid in dS (or quasi–dS) space, a large number of light modes also would pop up in the limit $\Lambda \to 0$, with Λ being positive.

The AdS-DC in de Sitter space provides a pathway, called the dark dimension scenario [7], to elucidate the origin of the cosmological hierarchy $\Lambda/M_p^4 \sim 10^{-122}$, because it connects the size of the compact space $R_\perp$ to the dark energy scale $\Lambda^{-1/4}$ via

$$R_\perp \sim \lambda \Lambda^{-1/4}, \tag{1}$$

where the proportionality factor is estimated to be within the range $10^{-1} < \lambda < 10^{-4}$. Actually, (1) derives from constraints by theory and experiment. On the one hand, since the associated Kaluza-Klein (KK) tower contains massive spin-two bosons, the Higuchi bound [8] sets an absolute

Published by the American Physical Society under the terms of the Creative Commons Attribution 4.0 International license. Further distribution of this work must maintain attribution to the author(s) and the published article's title, journal citation, and DOI. Funded by SCOAP³.

upper limit to the exponent of Λ^α, whereas explicit string calculations of the vacuum energy (see, e.g., [9–12]) yield a lower bound on α. All in all, the theoretical constraints lead to $1/4 \leq \alpha \leq 1/2$. On the other hand, experimental arguments (e.g., constraints on deviations from Newton's gravitational inverse-square law [13] and neutron star heating [14]) lead to the conclusion encapsulated in (1): The cosmological hierarchy problem can be addressed if there is one extra dimension of radius $R_\perp$ in the micron range and the lower bound for $\alpha = 1/4$ is basically saturated [7]. The Standard Model (SM) should then be localized on a D-brane transverse to the dark dimension [15]. A theoretical amendment on the connection between the cosmological and KK mass scales confirms $\alpha = 1/4$ [16]. Assembling all this together, we can further conclude that the KK tower of the new (dark) dimension opens up at the mass scale $m_{\rm KK} \sim 1/R_\perp$ at the eV range. Within this setup, the five-dimensional Planck scale (or species scale where gravity becomes strong [17–20]) is given by

$$M_* \sim m_{\rm KK}^{1/3} M_p^{2/3}, \tag{2}$$

where $M_p = 1/\sqrt{G_N}$ is the Planck mass, leading to $10^9 \lesssim M_*/\text{GeV} \lesssim 10^{10}$.

The dark dimension accumulates interesting phenomenology [21–39]. For example, it was noted by us [22] that primordial black holes (PBHs) with Schwarzschild radius smaller than a micron could be good dark matter candidates. A generalization to near-extremal black holes has been carried out in [38]. Complementary to the PBHs, it was observed in [25] that the universal coupling of the SM fields to the massive spin-two KK excitations of the graviton in the dark dimension provides an alternative dark matter contender. The cosmic evolution of the dark graviton gas is primarily dominated by "dark-to-dark" decays, yielding a specific realization of the dynamical dark matter framework [40]. An interesting close relation between PBHs and the dark gravitons has been pointed out in [24].

In this paper we provide new insights on PBHs as dark matter candidates. The layout is as follows. In Sec. II, we provide a concise overview of black hole evaporation within Hawking's semiclassical approximation. In Sec. III, we explore the impact of quantum effects, possibly associated with the memory burden, which could take the evaporation process out of the semiclassical regime by half-decay time [41–43]. In Sec. IV, we reassess limits on the abundance of PBHs as dark matter candidates, focusing on holes localized on the brane during the evaporation process. In Sec. V, we examine the possibility that bulk PBHs make the dark matter in the Universe. In Sec. VI, we consider a space with two boundaries for the dark dimension [44]. We study general phenomenological aspects of this construct, and in particular, we examine the possibility that the dark matter in the Universe is made of tubular-pancake shaped black holes localized on a brane, which is placed at the space boundary. The paper wraps up in Sec. VII with some conclusions.

II. SEMICLASSICAL BLACK HOLE EVAPORATION

In the mid-1970s Hawking pointed out that a black hole emits thermal radiation as if it were a blackbody, with a temperature inversely proportional to its mass [45,46]. In this section, we first review the main properties of Hawking evaporation of Schwarzschild black holes and of its generalization to dimension d. After that we review the evaporation of near-extremal black holes within the semiclassical approximation.

A. Schwarzschild black holes

It is well known that inertial observers in Minkowski space perceive the vacuum (the absence of particles), whereas observers moving with uniform proper acceleration a measure a thermal bath (thermal distribution of particles) of temperature $T = a/(2\pi)$ [47–49]. In special relativity, an observer moving with uniform proper acceleration through Minkowski spacetime is conveniently described with Rindler coordinates [50], which are related to the standard (Cartesian) Minkowski coordinates by $x = \rho \cosh\sigma$ and $t = \rho \sinh\sigma$. The line element in Rindler space is found to be

$$ds^2 = -\rho^2 d\sigma^2 + d\rho^2, \tag{3}$$

where $\rho = 1/a$ and where σ is related to the observer's proper time τ by $\sigma = a\tau$. Note that the local acceleration diverges as $\rho \to 0$.

By the same token, what inertial Schwarzschild observers measure as vacuum, the uniformly accelerated ones identify as thermal bath. The group of inertial Schwarzschild observers are the ones falling toward the black hole, while the uniformly accelerated observers are the ones who manage to keep constant distance from the event horizon, the acceleration being there to prevent the gravitational pull. This implies that black holes should have an approximate Rindler region near the horizon. More indicatively, consider the Schwarzschild metric

$$ds^2 = -(1 - r_s/r)dt^2 + (1 - r_s/r)^{-1}dr^2 + r^2 d\Omega_2^2, \tag{4}$$

where t is the universal time coordinate, r is the circumferential radius (defined so that the circumference of a sphere of radius r is $2\pi r$), $d\Omega_2$ is an interval of spherical solid angle, and $r_s = 2M_{\rm BH}$ is the horizon radius (in Planck units), with $M_{\rm BH}$ the black hole mass. The proper distance from the horizon is given by

$$\rho = \int_{r_s}^{r} \sqrt{g_{rr}(r')}dr' = \int_{r_s}^{r} \frac{dr'}{\sqrt{1-r_s/r}} = \sqrt{r(r-r_s)} + r_s \sinh\sqrt{r/r_s - 1}. \tag{5}$$

Substituting (5) into (4) the Schwarzschild metric can be recast as

$$ds^2 = -\left(1 - \frac{r_s}{r(\rho)}\right)dt^2 + d\rho^2 + r^2(\rho)d\Omega_2^2. \tag{6}$$

For $\delta/r_s \ll 1$, in the near-horizon limit, $r = r_s + \delta$, it follows that $\rho = 2\sqrt{r_s\delta}$. Bearing this in mind, the local metric to lowest order in δ is found to be

$$ds^2 = -\frac{\rho^2}{4r_s^2}dt^2 + d\rho^2 + r_s^2 d\Omega_2^2. \tag{7}$$

The (t,ρ) piece of this metric is Rindler space; we can rescale $t = 2r_s\sigma$ to make it look exactly like (3).

In analogy with Rindler space, the near-horizon observer must see the field excited at a local temperature

$$T = \frac{a}{2\pi} = \frac{1}{2\pi\rho} = \frac{1}{4\pi\sqrt{r_s r(1-r_s/r)}}. \tag{8}$$

The gravitational redshift is given by the square root of the time component of the metric. So for the field theory state to consistently extend, there must be a thermal background everywhere with the local temperature redshift matched to the near-horizon temperature

$$T(r') = \frac{1}{4\pi\sqrt{r_s r(1-r_s/r)}}\sqrt{\frac{1-r_s/r}{1-r_s/r'}} = \frac{1}{4\pi\sqrt{r_s r(1-r_s/r')}}. \tag{9}$$

The inverse temperature redshifted to r' at infinity is found to be

$$\lim_{r'\to\infty} T(r') = \frac{1}{4\pi\sqrt{r_s r}}. \tag{10}$$

For small δ, in the near-horizon limit

$$\lim_{r'\to\infty} T(r') = \frac{1}{4\pi r_s}. \tag{11}$$

All in all, a field theory defined on Schwarzschild background is in a thermal state whose Hawking temperature at infinity is given by

$$T_{\rm H} = \frac{1}{4\pi r_s}. \tag{12}$$

Armed with the Hawking temperature, we can now calculate the entropy of the black hole [51]. By adding a quantity of heat dQ the change in the black hole entropy is given by

$$dS_{\rm BH} = \frac{dQ}{T_{\rm H}} = 8\pi M_{\rm BH}\, dQ = 8\pi M_{\rm BH} dM_{\rm BH}, \tag{13}$$

where we assumed that the heat energy that enters serves to increase the total mass. The black hole entropy is then found to be

$$S_{\rm BH} = 2\pi M_{\rm BH} r_s. \tag{14}$$

Next, in line with our stated plan, we generalize the previous discussion to dimension d. Following [52], we conveniently work with the mass scale $M_d = [(2\pi)^{d-4}/(8\pi)]^{1/(d-2)}M_*$, where $M_p^2 = M_*^{d-2}(2\pi R_\perp)^{d-4}$ [15]. Throughout we rely on the probe brane approximation, which ensures that the only effect of the brane field is to bind the black hole to the brane. This is an adequate approximation provided $M_{\rm BH}$ is well above the brane tension, which is presumably of the order of but smaller than M_d. We also assume that the black hole can be treated as a flat d-dimensional object. This assumption is valid for extra dimensions that are larger than the d-dimensional Schwarzschild radius

$$r_s(M_{\rm BH}) \sim \frac{1}{M_d}\left(\frac{M_{\rm BH}}{M_d}\right)^{1/(d-3)}\left[\frac{2^{d-4}\pi^{(d-7)/2}\Gamma\left(\frac{d-1}{2}\right)}{d-2}\right]^{1/(d-3)}, \tag{15}$$

where $\Gamma(x)$ is the Gamma function [53–55]. Using (15) it is easily seen that, for dimension d, (12) and (14) generalize to

$$T_{\rm H} = \frac{d-3}{4\pi r_s} \tag{16}$$

and

$$S_{\rm BH} = \frac{4\pi M_{\rm BH} r_s}{d-2}, \tag{17}$$

respectively [56].

In the rest frame of the Schwarzschild black hole, both the average number [45,46] and the probability distribution of the number [57–59] of outgoing particles in each mode obey a thermal spectrum. However, in the neighborhood of the horizon, the black hole produces an effective potential barrier that backscatters part of the emitted radiation, modifying the thermal spectrum. The so-called "greybody

factors" σ_s, which controls the black hole absorption cross section, depends upon the spin of the emitted particles s, their energy Q, and $M_{\rm BH}$ [60–64]. The prevailing energies of the emitted particles are $\sim T_{\rm H} \sim 1/r_s$, resulting in s-wave dominance of the final state. This implies that the black hole evaporates with equal probability to a particle on the brane and in the compact space [65,66]. Thereby, the process of evaporation is driven by the large number of SM brane modes.

At high frequencies ($Qr_s \gg 1$) the greybody factors for each kind of particle must approach the geometrical optics limit. For exemplifying simplicity, in what follows we adopt the geometric optics approximation, and following [67], we conveniently write the greybody factors as a dimensionless constant, $\Gamma_s = \sigma_s/A_4$, normalized to the horizon surface area

$$A_4 = 4\pi\left(\frac{d-1}{2}\right)^{2/(d-3)}\frac{d-1}{d-3}r_s^2 \tag{18}$$

seen by the SM fields: $\Gamma_{s=0} = 1$, $\Gamma_{s=1/2} \approx 2/3$, and $\Gamma_{s=1} \approx 1/4$ [67].

The emission rate per degree of particle freedom i of particles of spin s with initial total energy between $(Q, Q+dQ)$ is found to be

$$\frac{d\dot{N}_i}{dQ} = \frac{\sigma_s}{8\pi^2}Q^2\left[\exp\left(\frac{Q}{T_{\rm H}}\right) - (-1)^{2s}\right]^{-1}. \tag{19}$$

The average total emission rate for particle species i is then

$$\dot{N}_i = f\frac{\Gamma_s}{32\pi^3}\frac{(d-1)^{(d-1)/(d-3)}(d-3)}{2^{2/(d-3)}}\Gamma(3)\zeta(3)T_{\rm H}, \tag{20}$$

where $\zeta(x)$ is the Riemann ζ function and $f = 1$ ($f = 3/4$) for bosons (fermions) [68]. For the different spins, the emission rate can be parametrized by

$$\dot{N}_i^{s=0} \sim 3.7\times 10^{18}\frac{(d-1)^{(d-1)/(d-3)}(d-3)}{2^{2/(d-3)}}\left(\frac{T_{\rm H}}{\rm MeV}\right)\ {\rm s}^{-1}, \tag{21}$$

$$\dot{N}_i^{s=1/2} \sim 1.8\times 10^{18}\frac{(d-1)^{(d-1)/(d-3)}(d-3)}{2^{2/(d-3)}}\left(\frac{T_{\rm H}}{\rm MeV}\right)\ {\rm s}^{-1}, \tag{22}$$

and

$$\dot{N}_i^{s=1} \sim 9.2\times 10^{17}\frac{(d-1)^{(d-1)/(d-3)}(d-3)}{2^{2/(d-3)}}\left(\frac{T_{\rm H}}{\rm MeV}\right)\ {\rm s}^{-1}. \tag{23}$$

The rate of change of the black hole mass in the evaporation process is estimated to be (i) for $d = 4$,

$$\left.\frac{dM_{\rm BH}}{dt}\right|_{\rm evap} = -\frac{M_p^2}{30720\pi M_{\rm BH}^2}\sum_i c_i(T_{\rm H})\tilde{f}\Gamma_s \sim -7.5\times 10^{-8}\left(\frac{M_{\rm BH}}{10^{16}\ {\rm g}}\right)^{-2}\sum_i c_i(T_{\rm H})\tilde{f}\Gamma_s {\rm g/s}, \tag{24}$$

and (ii) for $d = 5$,

$$\left.\frac{dM_{\rm BH}}{dt}\right|_{\rm evap} \sim -9\pi^{5/4}\zeta(4)T_{\rm H}^2\sum_i c_i(T_{\rm H})\tilde{f}\Gamma_s \sim -1.3\times 10^{-12}\left(\frac{M_{\rm BH}}{10^{16}\ {\rm g}}\right)^{-1}\sum_i c_i(T_{\rm H})\tilde{f}\Gamma_s {\rm g/s}, \tag{25}$$

where $c_i(T_{\rm H})$ counts the number of internal degrees of freedom of particle species i of mass m_i satisfying $m_i \ll T_{\rm H}$, $\tilde{f} = 1$ ($\tilde{f} = 7/8$) for bosons (fermions), and where, for $d = 5$, we have taken $M_* \sim 10^{10}$ GeV as expected in the dark dimension scenario [7]. A direct comparison of (24) and (25) shows that, for equal masses, five-dimensional (5D) Schwarzschild black holes evaporate slower than their 4D cousins. This is because 5D black holes are bigger and colder. Indeed, using (24) a straightforward calculation shows that 4D black holes with $M_{\rm BH} \gtrsim 5\times 10^{14}$ g can survive the age of the Universe, whereas for the dark dimension scenario we obtain

$$\tau_H \sim 13.8\left(\frac{M_{\rm BH}}{10^{12}\ {\rm g}}\right)^2\left(\frac{6}{\sum_i c_i(T_s)\tilde{f}\Gamma_s}\right)\ {\rm Gyr}. \tag{26}$$

A discussion of a 4D black hole evaporation entering the 5D regime together with details of the 4D to 5D transition is provided in the Appendix.

B. Near-extremal black holes

Next, we consider the Reissner-Nordström black hole in Einstein-Maxwell gravity, which is specified by its Arnowitt-Deser-Misner (ADM) mass $M_{\rm BH}$ and electric charge $Q_{\rm BH}$. The Einstein-Maxwell action in dimension d is given by

$$S_{\rm EM} = -\frac{1}{16\pi G}\int_M d^dx\sqrt{-g}(R - F^2), \tag{27}$$

where $F = dA$ and

$$A = -\sqrt{\frac{d-2}{2(d-3)}}\frac{q}{r^{d-3}}dt. \tag{28}$$

The d-dimensional Reissner-Nordström metric can be written as

$$ds^2 = -u(r)dt^2 + u^{-1}(r)dr^2 + r^2 d\Omega_{d-2}^2, \tag{29}$$

where

$$u(r) = 1 - \frac{m}{r^{d-3}} + \frac{q^2}{r^{2(d-3)}} \tag{30}$$

is the blackening function and

$$d\Omega_{d-2}^2 = d\chi_2^2 + \prod_{i=2}^{d-2} \sin^2\chi_i d\chi_{i+1}^2 \tag{31}$$

is the metric of a $(d-2)$-dimensional unit sphere, and where m is related to the ADM mass $M_{\rm BH}$ and q to the charge $Q_{\rm BH}$ of the black hole by

$$M_{\rm BH} = \frac{d-2}{16\pi G}\omega_{d-2} m \tag{32}$$

and

$$Q_{\rm BH} = \frac{\sqrt{2(d-2)(d-3)}}{8\pi G}\omega_{d-2} q, \tag{33}$$

with

$$\omega_{d-2} = \frac{2\pi^{(d-1)/2}}{\Gamma(\frac{d-1}{2})} \tag{34}$$

the volume of the unit $(d-2)$-sphere [69]. The black hole has two horizons located at the zeros of the blackening function, $u(r_\pm) = 0$, yielding

$$r_\pm = [(M_{\rm BH} + c)/M_d^{d-2}]^{1/(d-3)}, \tag{35}$$

where following [70] we conveniently introduce the extremality parameter

$$c = \sqrt{M_{\rm BH}^2 - Q_{\rm BH}^2 M_d^{d-2}} \sim M_{\rm BH}\sqrt{\beta/S_{\rm BH}}, \tag{36}$$

and where we have been cavalier on unimportant numerical factors taking $m \sim 2M_{\rm BH}/M_d^{d-2}$ and $q \sim Q_{\rm BH}/M_d^{d-2}$. To avoid naked singularities, we must require $M_{\rm BH}^2 \geq Q_{\rm BH}^2 M_d^{d-2}$.

Now, we define the temperature,

$$T_{\rm ne} \sim \frac{\beta^{1/2} T_{\rm H}}{S_{\rm BH}^{1/2}}, \tag{37}$$

where β is a factor of order one that controls the differences between $M_{\rm BH}$ and $Q_{\rm BH}$ [71]. By inspection of (36) and (37), we can see that near-extremal black holes are extremely cold due to the fact that $c/M_{\rm BH}$, which quantifies the near extremality, is extremely small because of the large entropy [38].

III. EFFECTS OF MEMORY BURDEN ON BLACK HOLE EVAPORATION

It was recently suggested [41–43] that quantum effects (e.g., memory burden) would take the evaporation process out of the semiclassical regime after about half-decay time has elapsed. It is this that we now turn to study. Actually, the black hole evaporation estimates presented in the previous section, based on the semiclassical approximation, rely on the assumption of self-similarity. Namely, we have assumed that, in the course of evaporation, a black hole gradually shrinks in size while maintaining the standard semiclassical relations between its parameters, such as its mass, the Schwarzschild radius, and the Hawking temperature. However, there have been some objections to this viewpoint, and actually arguments have been put forward suggesting the self-similarity assumption is inconsistent over the long timescales of the evolution.

The breakdown of self-similarity is deep rooted in the nature of entanglement. For a cavity emitting blackbody radiation, early on photon emission is entangled with atomic states in the cavity. However, once half the energy in the cavity is emitted, subsequent radiation emitted is entangled with radiation emitted earlier. As a result the entanglement entropy increases to some maximum, at about half the energy emitted, and then declines. A black hole may experience a similar behavior, because Hawking radiation is emitted from an entangled pair of photons or electron positron pairs. The Page time is defined by the condition that the mass of a black hole has decreased to half its original value via Hawking radiation, $\tau_{\rm half} \sim M_{\rm BH}/2$ [72,73]. Within this time, $r_s \to r_s/2$ and $S_{\rm BH} \to S_{\rm BH}/4$. It is at time $\sim\tau_{\rm half}$ when an observer that has configured a black hole with a set of known states on the horizon might find that they have been randomized beyond what can be recovered. In other words, information may remain encoded inside the black hole because the emitted radiation is thermal in character. However, after $\tau_{\rm half}$, the remaining black hole has only $1/4$ of its initial entropy and so much less information storage capacity. A far reaching proposal that can accommodate these ideas and describe the black hole evaporation for times $> \tau_{\rm half}$ is the so called "memory burden" effect, which insinuates that Hawking evaporation is slowed down by further n powers of the entropy $S_{\rm BH}$, after the Page time has elapsed [41–43,74].

It is not clear whether the memory burden effect still needs further justification and whether the black hole lifetime already gets increased after Page time, but herein we will explore its spectacular phenomenological consequences. Before proceeding, we pause to note that memory

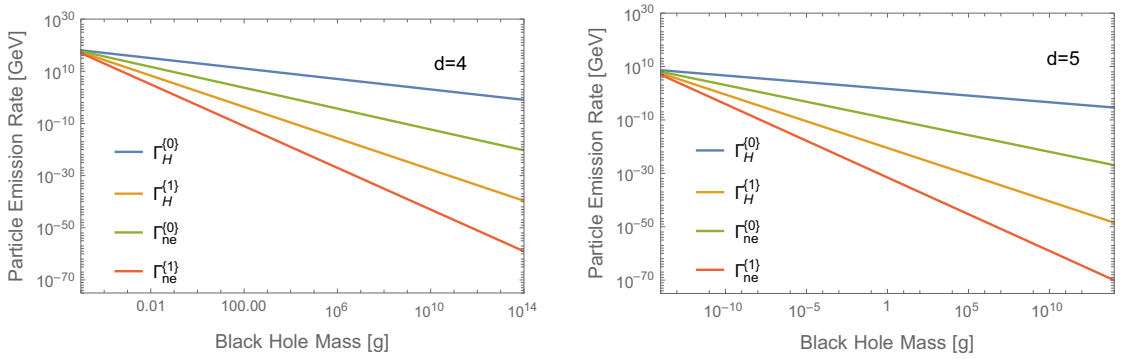

FIG. 1. Particle emission rate of Schwarzschild, near-extremal, and quantum black holes; for $d = 4$ (left) and $d = 5$ (right).

burden holds in any dimension and herein we assume that the behavior of $t_{\rm half}$ is roughly universal for any dimension.

Bearing this in mind, a comparison of the scaling behavior of the different rates of particle emission is of interest. The scaling behavior of the semiclassical decay rate ($\dot{N}_i \equiv \Gamma_{\rm H}^{\{0\}}, \ \forall \ i$) of a Schwarzschild black hole in dimension d follows from (20). Neglecting the effect of greybody factors and mass thresholds we have

$$\Gamma_{\rm H}^{\{0\}} \sim T_{\rm H} \sim M_d S_{\rm BH}^{-1/(d-2)} \sim M_d \left(\frac{M_{\rm BH}}{M_d}\right)^{-1/(d-3)}. \quad (38)$$

The quantum decay rate has an additional suppression (compared to the Hawking decay rate),

$$\Gamma_{\rm H}^{\{n\}} \sim \frac{T_{\rm H}}{S_{\rm BH}^n} \sim M_d S_{\rm BH}^{(-1-nd+2n)/(d-2)} \sim M_d \left(\frac{M_{\rm BH}}{M_d}\right)^{(-1-nd+2n)/(d-3)}, \quad (39)$$

and the suppression factor $1/S_{\rm BH}^n \sim (M_{\rm BH}/M_d)^{(-nd+2n)/(d-3)}$ is dimension dependent. Throughout, n is a non-negative integer parametrizing the quantum suppression when the black hole enters the memory burden phase.

For near-extremal black holes, the semiclassical decay rate in dimension d is suppressed compared to the Schwarzschild decay rate by a factor $1/S_{\rm BH}^{1/2}$ [38],

$$\Gamma_{\rm ne}^{\{0\}} \sim \frac{\beta^{1/2} T_{\rm H}}{S_{\rm BH}^{1/2}} \sim \beta^{1/2} M_d S_{\rm BH}^{-d/(2d-4)} \sim \beta^{1/2} M_d \left(\frac{M_{\rm BH}}{M_d}\right)^{-d/(2d-6)}. \quad (40)$$

The quantum decay rate of a near-extremal black hole in dimension d gets again an additional suppression compared to the near-extremal Hawking decay rate by a factor $1/S_{\rm BH}^n$,

$$\Gamma_{\rm ne}^{\{n\}} \sim \frac{\beta^{1/2} T_{\rm H}}{S_{\rm BH}^{n+1/2}} \sim \beta^{1/2} M_d S_{\rm BH}^{(-d/2-nd+2n)/(d-2)} \sim \sqrt{\beta} M_d \left(\frac{M_{\rm BH}}{M_d}\right)^{(-d/2-nd+2n)/(d-3)}. \quad (41)$$

In Fig. 1 we show a comparison of the various decay rates. For large masses (or equivalently large entropies), the quantum decay rates are suppressed by several orders of magnitude. The difference, of course, is reduced with decreasing entropy, and all the decay rates become equal at the minimum black hole mass $M_{\rm BH,min} \sim M_d$.

In summary, Hawking's semiclassical approximation applied to 5D black holes perceiving the dark dimension scenario gives very robust predictions and leads to reliable conclusions. More spectacular results can be obtained adopting the black hole portrait endowed with the memory burden. However, the theoretical underpinning and the precise implementation of the memory burden is rather speculative. In particular, via memory burden the black hole decay rate gets dramatically changed already after Page time, whereas it also could be conceivable that quantum effects affect the black hole decay rate at much later timescales. Therefore, it will be very interesting to provide further theoretical evidence for memory burden associated closer to the entanglement island approach [75–85].

IV. PRIMORDIAL BLACK HOLES AS DARK MATTER

Since the late 1960s there has been speculation suggesting that black holes could be formed from the collapse of large amplitude fluctuations in the early Universe [86–89]. An order of magnitude estimate of $M_{\rm BH}$ can be obtained by equating the scaling of the cosmological energy density with time t in the radiation dominated epoch,

$$\rho \sim M_p^2/t^2, \quad (42)$$

to the required density in a region of mass $M_{\rm BH}$ that is able to collapse within its Schwarzschild radius

$$\rho \sim M_p^6/M_{\rm BH}^2. \tag{43}$$

Linking (42) and (43) gives the idea that at production PBHs would have roughly the cosmological horizon mass [90]

$$M_{\rm BH} \sim tM_p^2 \sim 10^{15}\left(\frac{t}{10^{-23}\ \rm s}\right)\ \rm g. \tag{44}$$

Now, it is straightforward to see that a black hole would have the Planck mass ($M_p \sim 10^{-5}$ g) if it formed at the Planck time (10^{-43} s), $1M_\odot$ if it formed at the QCD epoch (10^{-5} s), and $10^5 M_\odot$ if it formed at $t \sim 1$ s, comparable to the mass of the holes thought to reside in Galactic nuclei. The back-of-the-envelope calculation yielding (44) hints that PBHs could span an enormous mass range. Even though the spectrum of masses of these PBHs has yet to see the light of day, on cosmological scales they would behave like a typical cold dark matter particle.

First of all, an all-dark-matter interpretation in terms of PBHs, namely, the possible mass range for PBHs is constrained by the requirement that they must have survived up today, i.e., PBHs must have lived longer than the age of the Universe. Additional severe constraints are provided by several observations [90–93]. To be specific, the extragalactic γ-ray background [94], cosmic microwave background (CMB) [95], 511 keV γ-ray line [96–99], EDGES 21-cm signal [100], and MeV Galactic diffuse emission [101–103] constrain evaporation of black holes with masses $\lesssim 10^{17}$ g, whereas the nonobservation of microlensing events by MACHO [104], EROS [105], Kepler [106], Icarus [107], OGLE [108], and Subaru-HSC [109] set an upper limit on the black hole abundance for masses $M_{\rm BH} \gtrsim 10^{21}$ g.

Before proceeding, we pause and call attention to a captivating coincidence,

$$\text{size of the dark dimension} \sim \text{wavelength of visible light}, \tag{45}$$

which implies that the Schwarzschild radius of 5D black holes is well below the wavelength of light. For pointlike lenses, this is precisely the critical length where geometric optics breaks down and the effects of wave optics suppress the magnification, obstructing the sensitivity to 5D PBH microlensing signals [109]. So 5D PBHs escape these microlensing constraints; at the same time, as pointed out in [22], they are longer-lived than their 4D counter parts, and this makes them more promising all-dark-matter candidates.

In light of the stunning coincidence (45), hereafter we will now focus on the bounds imposed by the extragalactic γ-ray background [94], CMB spectrum [95], 511 keV γ-ray line [96,97], and MeV Galactic diffuse emission [101–103] which directly constrain the black hole decay rate. As previously noted, these constraints place an upper limit on the dark matter fraction $f_{\rm PBH}$ composed of PBHs.

Before proceeding, we pause to note that femtolensing of cosmological gamma-ray bursts (GRBs) could be used to search for PBHs in the mass range $10^{17} \lesssim M_{\rm BH}/\rm g \lesssim 10^{20}$ [110]. The lack of femtolensing detection by the Fermi Gamma-ray burst monitor was used to constrain PBHs with mass in the range $10^{17.7} < M_{\rm BH}/\rm g \lesssim 10^{20}$ to contribute no more than 10% to the total dark matter abundance [111]. However, the validity of this GRB constraint has been called into question, because it is based on the assumption that the gamma-ray source is pointlike in the lens plane [112]. The nonpointlike nature of GRBs implies that most of them are too big when projected onto the lens plane to yield meaningful femtolensing limits. Indeed, only a small GRB population with very fast variability might be suitable for PBH searches. When this systematic effect is taken into consideration to decontaminate the Fermi sample, the GRB constraint on PBHs becomes obsolete. A sample of 100 GRBs with transverse size 10^9 cm would be needed to probe the 5D PBHs [112].

Black hole evaporation has two main channels contributing to the (diffuse) isotropic γ-ray flux: (i) direct photon emission and (ii) positron emission (these positrons annihilate with thermal electrons producing an x-ray background at energies around and below 511 keV). The diffuse photon emission consists of a contribution from PBHs from extragalactic structures at all redshifts. Limits on $f_{\rm PBH}$ are obtained by demanding that the emission from PBH evaporation does not exceed the x-ray and soft γ-ray isotropic fluxes, neither the Galactic intensity associated with the line-of-sight integrated Navarro-Frenk-White dark matter density profile [113]. Observations of the diffuse γ-ray emission in the direction of the Galactic Center offer the best and most solid constraints of $f_{\rm PBH}$ [103].

The upper panel of Fig. 2 shows the constraints on the PBH fraction in the mass range of interest for $d = 4$. The concomitant constraints for $d = 5$ can be estimated by a simple rescaling procedure. The central idea to decipher the change of scale is that, for a given photon energy, or equivalently, a given Hawking temperature, it is reasonable to expect a comparable limit on $f_{\rm PBH}$ for both $d = 4$ and $d = 5$, i.e.,

$$\rho^{4D}_{\rm PBH}(T_{\rm H}) \sim \rho^{5D}_{\rm PBH}(T_{\rm H}). \tag{46}$$

Note that at given $T_{\rm H}$, the required PBH number density in 5D is larger than the one in 4D

$$n^{4D}_{\rm PBH}(T_{\rm H}) < n^{5D}_{\rm PBH}(T_{\rm H}), \tag{47}$$

but this is automatically compensated by the fact that at fixed Hawking temperature the 5D black holes have smaller $M_{\rm BH}$ than those in 4D, i.e.,

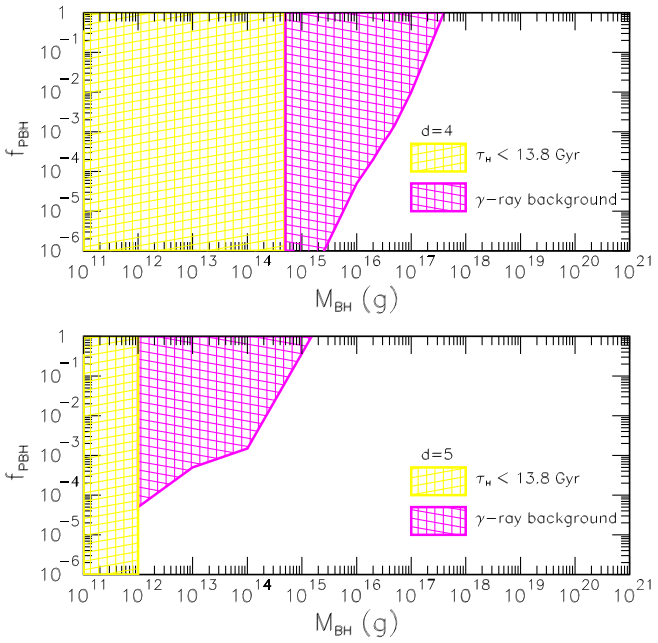

FIG. 2. Constraints on $f_{\rm PBH}$ as a function of the PBH mass $M_{\rm BH}$, assuming a monochromatic mass function. The yellow area indicates the region where black holes do not survive the age of the Universe. The region shaded in magenta corresponds to the upper limits from the extragalactic γ-ray background [94], CMB spectrum [95], 511 keV γ-ray line [96,97], and MeV Galactic diffuse emission [101–103]. The upper panel shows the results for $d = 4$ and the lower panel for $d = 5$.

$$M_{\rm BH}^{4D}(T_{\rm H}) > M_{\rm BH}^{5D}(T_{\rm H}), \tag{48}$$

yielding equal density.

For example, in $d = 4$, the Hawking temperature is related to the mass of the black hole by [99]

$$T_H = \frac{M_p^2}{8\pi M_{\rm BH}} \sim \left(\frac{M_{\rm BH}}{10^{16}\ {\rm g}}\right)^{-1}\ {\rm MeV}, \tag{49}$$

whereas in $d = 5$ the Hawking temperature mass relation is found to be

$$T_H \sim 1/r_s \sim \left(\frac{M_{\rm BH}}{10^{12}\ {\rm g}}\right)^{-1/2}\ {\rm MeV}, \tag{50}$$

where we have taken $M_d \sim 10^{10}$ GeV.[1] This means that since $f_{\rm PBH} \lesssim 5 \times 10^{-5}$ in $d = 4$ for $M_{\rm BH} \sim 10^{16}$ g, our reasoning indicates that $f_{\rm PBH} \lesssim 5 \times 10^{-5}$ for $M_{\rm BH} \sim 10^{12}$ g in $d = 5$. The complete rescaling of $f_{\rm PBH}$ for the $M_{\rm BH}$ range of interest is displayed in the lower panel of Fig. 2.

In Sec. III we have seen that near-extremal black holes are extremely cold. For example, a black hole of $M \sim 10^5$ g has a temperature $T_H \sim 4$ GeV. Substituting these figures into (24) we find that the Hawking lifetime of a 10^5 g Schwarzschild black hole is $\tau_H \sim 4 \times 10^{-5}$ yr. For a near-extremal black hole of the same mass, using (37) we find that its temperature would be $T_{\rm ne} \sim 10^{-5}\sqrt{\beta}$eV, and so using (26) its lifetime $\tau_{\rm ne} \sim 15/\sqrt{\beta}$Gyr. Note that the energy of the emitted particles by the near-extremal black hole is well below the peak of the CMB photons. We can conclude that, if there were 5D primordial near-extremal black holes in nature, then a PBH all-dark-matter interpretation would be possible in the mass range

$$10^5\sqrt{\beta} \lesssim M/{\rm g} \lesssim 10^{21}. \tag{51}$$

Of course, by tuning the β parameter we can have a PBH all-dark-matter interpretation with very light 5D black holes.[2]

Next, we explore how the memory burden effect impacts the mass range of a PBH all-dark-matter interpretation. Memory burden dramatically enhances the black hole lifetime and implies that *a priori* the bounds from the age of the Universe are much milder than compared to those from the semiclassical black hole decay. However, photon emission will put additional constraints, which we will discuss in the following. To be specific, we assume only two phases in the evaporation process: semiclassical evaporation up to $\tau_{\rm half}$ followed by a quantum regime characterized by $n = 1$. We can duplicate the procedure adopted above to derive the allowed mass range for a PBH all-dark-matter interpretation. For $d = 4$, the memory burden effect opens a new window in the mass range $10^9 \lesssim M_{\rm BH}/{\rm g} \lesssim 10^{10}$ [115]. This corresponds to PBHs with temperatures $1 \lesssim T_H/{\rm TeV} \lesssim 10$. The corresponding 5D mass range for the same temperature interval is $10^{-2} \lesssim M_{\rm BH}/{\rm g} \lesssim 1$. Imposing the $S_{\rm BH}$ enhancement on (26), we find that

$$\tau_{\rm H}^{\{1\}} \sim 4 \times 10^{17}\left(\frac{M_{\rm BH}}{5\ {\rm g}}\right)^2\ {\rm s}, \tag{52}$$

i.e., black holes could survive the age of the Universe if $M_{\rm BH} \gtrsim 5$ g. Bounds on the black hole abundance as a function of the initial black hole mass are encapsulated in Fig. 3. We conclude that within the dark dimension scenario the memory burden effect with $n = 1$ does not open any new window that could allow an all-dark-matter interpretation composed of primordial black holes.

[1]We adopt the highest value of M_d to remain conservative in the estimated bound on $f_{\rm PBH}$.

[2]The possibility of 4D near-extremal black holes making the dark matter was suggested in [114].

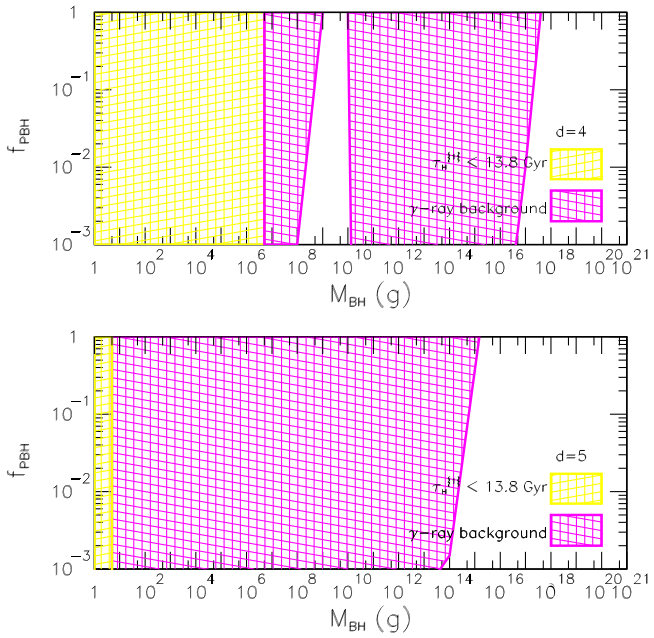

FIG. 3. Constraints on $f_{\rm PBH}$ as a function of the PBH mass $M_{\rm BH}$, assuming a monochromatic mass function. The yellow area indicates the region where black holes do not survive the age of the Universe, i.e., $\tau_{\rm H}^{\{1\}} < 13.8$ Gyr. The region shaded in magenta corresponds to the upper limits from the extragalactic γ-ray background [94], CMB spectrum [95], 511 keV γ-ray line [96,97], and the MeV Galactic diffuse emission [101–103]. The upper panel shows the results for $d = 4$ and the lower panel for $d = 5$.

V. BLACK HOLES LOCALIZED IN THE BULK

Hitherto, we have assumed that 5D black holes stay attached to the brane during the evaporation process. In this section we relax this assumption and allow them wander off into the bulk. Without knowing more details of the bulk and brane theory it is not worth considering to calculate the probability of such wandering in detail. However, we can assume that the holes are out of the brane world and study the evaporation effects of these bulk PBHs. Furthermore, it is always possible that the PBHs are produced in the bulk to start with. This situation will be more appealing within the proposal introduced elsewhere [26,35], in which we postulated that the dark dimension may have undergone a uniform rapid expansion, together with the three-dimensional noncompact space, by regular exponential inflation driven by an (approximate) higher-dimensional cosmological constant. If this were the case, then primordial fluctuations during inflation of the compact space could lead to the production of black holes in the bulk. In this section we then assume that PBHs are localized or propagating in the bulk.

Bulk black holes live longer than those attached to the brane. This is because KK modes are excitations in the full transverse space and so their overlap with small (higher-dimensional) black holes is suppressed by the geometric factor $(r_s/R_\perp)^{d-4}$ relative to the brane fields. This geometric suppression precisely compensates for the enormous number of modes and the total KK contribution is only of same order as that from a single brane field [65]. Actually, greybody factors suppress graviton emission when compared to fermions and gauge bosons, and hence bulk black holes that do not have access to the brane degrees of freedom are expected to live longer. In addition, since there is no emission on the brane the bounds due to photon evaporation can be avoided. This implies that PBHs localized in the bulk can provide an all-dark-matter interpretation if

$$10^{11} \lesssim M_{\rm BH}/{\rm g} < 10^{21}, \tag{53}$$

where we have remained conservative, and following [67] we assumed that the ratio of the emitted flux into a single brane field over a single bulk field is roughly a factor of 2.

We note that within the black hole memory burden an all-dark-matter interpretation is almost unconstrained, and so the allowed mass range estimate given in (53) can be extended down to $1 \lesssim M_{\rm BH}/{\rm g} \lesssim 10^{21}$. Actually, the minimum black hole mass can be further reduced by advocating a multiple-phase black hole evolution, such that in each phase there is a $1/S_{\rm BH}$ increase in the memory burden suppression factor of the decay rate.

VI. THE DARK DIMENSION AS A SPACE WITH TWO BOUNDARIES

Very recently, it was conjectured that the dark dimension can also be viewed as a line interval with end-of-the-world nine-branes attached at each end [44]. In this section, we briefly comment on the impact that this thought-provoking viewpoint could have on phenomenological aspects of the dark dimension scenario.

Actually, the line interval along the dark dimension y can also be understood as a semicircular dimension endowed with $S^1/\mathbb{Z}_2$ symmetry. This symmetry has radical consequences for models in which neutrino masses originate in three 5D Dirac fermions Ψ_α, which are singlets under the SM gauge symmetries and interact in our brane with the three active left-handed neutrinos $\nu_{\alpha L}$ in a way that conserves lepton number, where the indices $\alpha = e, \mu, \tau$ denote the generation [116–118]. In the Weyl basis, each Dirac field can be decomposed into two two-component spinors $\Psi_\alpha \equiv (\psi_{\alpha L}, \psi_{\alpha R})^T$. Now, the $\mathbb{Z}_2$ symmetry of $S^1/\mathbb{Z}_2$ contains y to $-y$ which acts as chirality (γ_5) on spinors. This implies that one of the two-component Weyl spinors, say $\psi_{\alpha R}$, would be even under $\mathbb{Z}_2$, while the other spinor $\psi_{\alpha L}$ would be odd. If $\nu_{\alpha L}$ are restricted to the brane located at the fixed point $y = 0$, then $\psi_{\alpha L}$ vanishes at this point and so the coupling is between $\nu_{\alpha L}$ and $\psi_{\alpha R}$. As we have shown

elsewhere [37], the model remains consistent with experiment because only the $\psi_{\alpha R}$ degrees of freedom contribute to the effective number of equivalent neutrino species $N_{\rm eff}$.

Two different types of PBHs can be produced if the dark dimension is seen as space with two boundaries: (i) 5D Schwarzschild black holes that propagate freely (or else are localized) in the bulk and (ii) tubular-pancake shaped black holes, which are bound to a brane localized at the boundary of space. The second type of black holes would resemble the black cigars described in [119], and therefore far away from the space boundary the black hole metric on the end-of-the-world brane would be approximately Schwarzschild. In the spirit of [120], we argue that the phenomenology of these black cigars is similar to that of the 5D Schwarzschild black holes discussed throughout this paper. This implies that primordial black cigars could provide an all-dark-matter interpretation for masses in the range $10^{15} < M_{\rm BH}/{\rm g} < 10^{21}$; see Fig. 2 for details. We have estimated in the previous section that to accommodate the observed dark matter density Schwarzschild black holes living in the bulk should have masses in the range $10^{11} \lesssim M_{\rm BH}/{\rm g} < 10^{21}$.

We have stressed in the Introduction that the dark graviton gas proposal requires KK excitations that are unstable [25]. Actually, there are strong bounds on the changing dark matter density that imply that the decays to lighter gravitons of the KK tower must not lose much mass to kinetic energy [36]. A typical violation of KK quantum number δ_n cannot be too large and requires $\delta_n \sim \mathcal{O}(1)$. The proposal entertained in [44] provides a profitable arena to accommodate the dark graviton gas cascade, because $S^1/\mathbb{Z}_2$ automatically breaks the $U(1)$ isometry associated with the KK momentum conservation. Indeed, for $S^1/\mathbb{Z}_2$ there are two level sources of KK momentum violation:

(i) KK momenta are conserved modulo 2;
(ii) KK states decay to brane states with a coupling that falls off exponentially at large KK number $n > M/m_{\rm KK}$ with M the brane width. This of course feeds back to a momentum violation among KK modes by a loop of brane states.

Now, the KK momentum violation can leave a discrete $\mathbb{Z}_2$ symmetry acting as the KK number parity. This symmetry can be, in principle, implemented to brane states, opening the possibility for alternative dark matter candidates, such as the radion or the lightest odd KK in the presence of KK parity symmetry. For example, in [34] we assume that no such discrete symmetry survives and KK modes decay to the radion. In this model we can avoid the velocity kick constraints on KK momentum violation because the graviton tower decays into the radion before primordial nucleosynthesis. It is of interest to see whether it is possible to translate the KK momentum violation effects into an effective δ_n. We plan to elaborate on this idea in future publications.

VII. CONCLUSIONS

We have shown that 5D black holes perceiving the dark dimension are bigger, colder, and longer-lived than usual 4D black holes of the same mass. Adopting the robust Hawking semiclassical approximation, we have demonstrated that a PBH all-dark-matter interpretation would be possible for the following mass ranges:

(i) Schwarzschild black holes localized on the brane $\Rightarrow 10^{15} < M_{\rm BH}/{\rm g} < 10^{21}$;
(ii) Schwarzschild black holes localized in the bulk $\Rightarrow 10^{11} \lesssim M_{\rm BH}/{\rm g} < 10^{21}$;
(iii) near-extremal black holes localized on the brane $\Rightarrow 10^{5}\sqrt{\beta} < M_{\rm BH}/{\rm g} < 10^{21}$;

where β measures the near-extremality. The more speculative memory burden effect, with decay rate suppressed by $1/S_{\rm BH}$, could only extend this mass range if black holes are localized on the bulk. Finally, we have argued that the mass ranges given above for a PBH dark matter interpretation would not be modified if one assumes a space with two boundaries for the dark dimension.

ACKNOWLEDGMENTS

We thank Gia Dvali, Elias Kiritsis, and Georges Obied for discussion. The work of L. A. A. is supported by the U.S. National Science Foundation (NSF Grant No. PHY-2112527). I. A. is supported by the Second Century Fund (C2F), Chulalongkorn University. The work of D. L. is supported by the Origins Excellence Cluster and by the German-Israel-Project (DIP) on Holography and the swampland.

APPENDIX: TRANSITION BETWEEN 4D⇋5D BLACK HOLES AND RELATED SPECIES DESCRIPTION

In this appendix, we compare the differences in the change of the black hole lifetime for the following two scenarios: (i) addition of KK graviton towers that inevitably emerge when the 4D spacetime is endowed with compact space and (ii) a 4D effective theory with N massless species (but without reference to higher dimensions).

We first recapitulate the properties of higher-dimensional black holes. From (15), the Schwarzschild radius of a d-dimensional black hole scales as $r_s \sim M_{\rm BH}^{1/(d-3)}/M_d^{(d-2)/(d-3)}$, where $M_d \sim m_{\rm KK}^{(d-4)/(d-2)} M_p^{2/(d-2)}$ is the 5D Planck scale and $m_{\rm KK}$ is the KK mass scale. The species scale can be rewritten in terms of the number of KK species N as $M_d \sim M_p N^{-1/2}$ and we can also express N in terms of the KK mass, yielding $N \sim (M_p/m_{\rm KK})^{2(d-4)/(d-2)}$. Putting these formulas together r_s can be rewritten in terms of N as $r_s \sim (M_{\rm BH}^{1/(d-3)}/M_p^{(d-2)/(d-3)}) N^{(d-2)/(2d-6)}$ and we see that r_s scales with a positive power of N. For example, for the dark dimension scenario (with $d = 5$), one gets

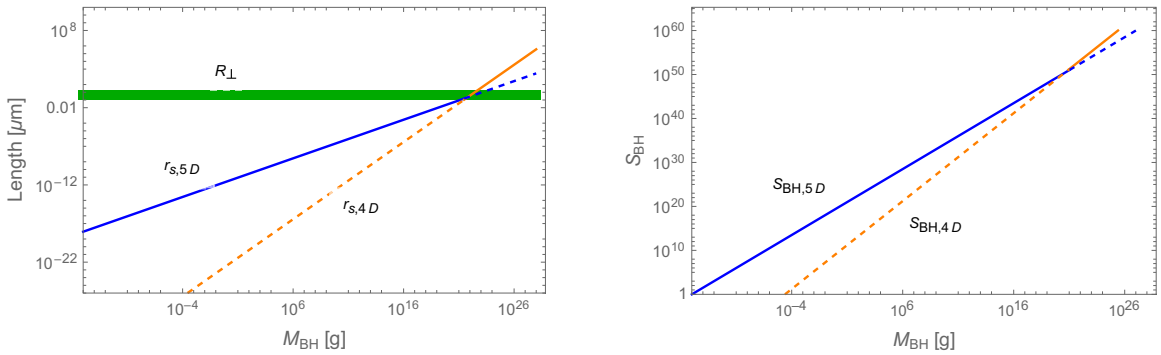

FIG. 4. Scaling of the Schwarzschild radius (left) and black hole entropy (right) in $d = 4$ and $d = 5$ dimensions.

$$r_s = M_{\rm BH}^{1/2} M_p^{-3/2} N^{3/4} = M_{\rm BH} M_p^{-2} (M_p/M_{\rm BH})^{1/2} N^{3/4}, \quad \text{(A1)}$$

where the term $(M_p/M_{\rm BH})^{1/2} N^{3/4}$ is the enhancement factor of the Schwarzschild radius compared to the 4D case. For the dark dimension, $N \sim 10^{18}$ and $(M_p/M_{\rm BH}) \sim 10^{-19}$ for $M_{\rm BH} \sim 10^{14}$ g. Thus, we see that the radius is increased compared to the 4D case.

Next, we calculate the Hawking decay time $\tau_{\rm H} \sim S_{\rm BH} r_s$, where the entropy is

$$S_{\rm BH} \sim M_{\rm BH} r_s \sim (M_{\rm BH}/M_d)^{(d-2)/(d-3)}. \quad \text{(A2)}$$

Thus, putting all this together, we obtain $\tau_{\rm H} = (M_{\rm BH}^{(d-1)/(d-3)}/M_d^{(2d-4)/(d-3)}) N^{(d-2)/(d-3)}$, which scales with a positive power of N. For example, for the dark dimension (with $d = 5$), it follows that

$$\tau_{\rm H} \sim M_{\rm BH}^2 M_p^{-3} N^{3/2} = M_{\rm BH}^3 M_p^{-4} (M_p/M_{\rm BH}) N^{3/2}, \quad \text{(A3)}$$

where the term $(M_p/M_{\rm BH}) N^{3/2}$ is the enhancement factor of the black hole lifetime compared to the 4D case.

Now, consider a 4D effective theory with N species (and no reference to higher dimensions). The minimal black hole radius is set by the species length, $r_{\rm min} = 1/M_d = \sqrt{N} l_p$, with $l_p \sim 1/M_p$ [71]. The corresponding minimal mass is $M_{\rm BH,min} = r_{s,\rm min} M_p^2 = \sqrt{N} M_p$, and the corresponding entropy is $S_{\rm BH,min} = r_{s,\rm min}^2 M_p^2 = N$. Finally, the maximal temperature, which sets the semiclassical decay rate, is $T_{\rm H,max} = 1/r_{s,\rm min} = M_d = M_p/\sqrt{N}$. We can now calculate the lifetime of the minimal black hole,

$$\tau_{\rm H,min} = r_{s,\rm min} S_{\rm BH,min} = N^{3/2} l_p, \quad \text{(A4)}$$

and see that it has increased with respect to the lifetime of the minimal black hole we would have obtained in the absence of N. However, it is important to stress that this enhancement is in essence different from the one associated with the KK towers, because we are not comparing black holes of the same mass, i.e., the minimal black hole in a 4D theory with species is heavier than the one in the absence of N. For equal black hole masses, the rate of decay in a theory with species is increased N-fold. As a consequence, the Hawking decay time in the presence of species is shortened to [43]

$$\tau_{\rm H} \sim r_s S_{\rm BH}/N. \quad \text{(A5)}$$

To understand the difference between the two scenarios, we can compare (A2) with the black hole entropy

$$S_{\rm BH} \sim (M_{\rm BH}/M_p)^2, \quad \text{(A6)}$$

of a 4D effective theory with N species but without compact dimensions. Setting $d = 5$ and using $M_p^2 \sim M_d^3 R_\perp$ we recast (A2) as

$$S_{\rm BH} \sim M_{\rm BH}^{3/2} R_\perp^{1/2}/M_p. \quad \text{(A7)}$$

In Fig. 4 we show a comparison of the 4D and 5D scaling behavior of the black hole entropy as given by (A6) and (A7). We can conclude that, when considering a 4D theory with addition of N species, the black hole formulas do not change in essence, but there are more channels for the evaporation process. For example, we can compare the evaporation of a black hole into SM fields and its minimal extension when the theory is extended by three right-handed Dirac neutrinos. If the black hole can emit right-handed neutrinos, it would have a shorter lifetime than if it only emits SM degrees of freedom. The minimum black hole mass available in the SM extension is increased, because the black hole must store extra information, this is all. Now, by adding species in a higher-dimensional theory, it follows from (A6) and (A7) that the scaling behavior of the entropy changes and for the black hole it is more convenient to be in

the 5D configuration because it has more entropy than the 4D configuration. As can be seen in Fig. 4, for $R_\perp \sim 1$ μm, the transition takes place at $M_{\rm BH} \sim 10^{21}$ g. Note that the two entropies in (A6) and (A7) are equal at the 5D–4D transition point where $M_{\rm BH} = M_p^2 R_\perp$. Moreover, the entropy crosses the horizontal axis where the black hole masses are the same as the 4D or 5D Planck masses. Then, the associated lengths are the 4D or 5D Planck lengths, where the two entropies are equal to 1.[3]

[3]The phase transition between 4D and 5D black holes was also recently investigated in [121].

[1] C. Vafa, The string landscape and the swampland, arXiv:hep-th/0509212.
[2] M. van Beest, J. Calderón-Infante, D. Mirfendereski, and I. Valenzuela, Lectures on the swampland program in string compactifications, Phys. Rep. **989**, 1 (2022).
[3] E. Palti, The swampland: Introduction and review, Fortschr. Phys. **67**, 1900037 (2019).
[4] N. B. Agmon, A. Bedroya, M. J. Kang, and C. Vafa, Lectures on the string landscape and the swampland, arXiv:2212.06187.
[5] H. Ooguri and C. Vafa, On the geometry of the string landscape and the swampland, Nucl. Phys. **B766**, 21 (2007).
[6] D. Lüst, E. Palti, and C. Vafa, AdS and the swampland, Phys. Lett. B **797**, 134867 (2019).
[7] M. Montero, C. Vafa, and I. Valenzuela, The dark dimension and the swampland, J. High Energy Phys. 02 (2023) 022.
[8] A. Higuchi, Forbidden mass range for spin-2 field theory in de Sitter space-time, Nucl. Phys. **B282**, 397 (1987).
[9] H. Itoyama and T. R. Taylor, Supersymmetry restoration in the compactified $O(16) \times O(16)$-prime heterotic string theory, Phys. Lett. B **186**, 129 (1987).
[10] H. Itoyama and T. R. Taylor, Small cosmological constant in string models, Report No. FERMILAB-CONF-87-129-T.
[11] I. Antoniadis and C. Kounnas, Superstring phase transition at high temperature, Phys. Lett. B **261**, 369 (1991).
[12] Q. Bonnefoy, E. Dudas, and S. Lüst, On the weak gravity conjecture in string theory with broken supersymmetry, Nucl. Phys. **B947**, 114738 (2019).
[13] J. G. Lee, E. G. Adelberger, T. S. Cook, S. M. Fleischer, and B. R. Heckel, New test of the gravitational $1/r^2$ law at separations down to 52 μm, Phys. Rev. Lett. **124**, 101101 (2020).
[14] S. Hannestad and G. G. Raffelt, Supernova and neutron star limits on large extra dimensions reexamined, Phys. Rev. D **67**, 125008 (2003); **69**, 029901(E) (2004).
[15] I. Antoniadis, N. Arkani-Hamed, S. Dimopoulos, and G. R. Dvali, New dimensions at a millimeter to a Fermi and superstrings at a TeV, Phys. Lett. B **436**, 257 (1998).
[16] L. A. Anchordoqui, I. Antoniadis, D. Lüst, and S. Lüst, On the cosmological constant, the KK mass scale, and the cut-off dependence in the dark dimension scenario, Eur. Phys. J. C **83**, 1016 (2023).
[17] G. Dvali, Black holes and large N species solution to the hierarchy problem, Fortschr. Phys. **58**, 528 (2010).
[18] G. Dvali and M. Redi, Black hole bound on the number of species and quantum gravity at LHC, Phys. Rev. D **77**, 045027 (2008).
[19] N. Cribiori, D. Lüst, and G. Staudt, Black hole entropy and moduli-dependent species scale, Phys. Lett. B **844**, 138113 (2023).
[20] D. van de Heisteeg, C. Vafa, M. Wiesner, and D. H. Wu, Species scale in diverse dimensions, J. High Energy Phys. 05 (2024) 112.
[21] L. A. Anchordoqui, Dark dimension, the swampland, and the origin of cosmic rays beyond the Greisen-Zatsepin-Kuzmin barrier, Phys. Rev. D **106**, 116022 (2022).
[22] L. A. Anchordoqui, I. Antoniadis, and D. Lüst, Dark dimension, the swampland, and the dark matter fraction composed of primordial black holes, Phys. Rev. D **106**, 086001 (2022).
[23] R. Blumenhagen, M. Brinkmann, and A. Makridou, The dark dimension in a warped throat, Phys. Lett. B **838**, 137699 (2023).
[24] L. A. Anchordoqui, I. Antoniadis, and D. Lüst, The dark universe: Primordial black hole $\leftrightharpoons$ dark graviton gas connection, Phys. Lett. B **840**, 137844 (2023).
[25] E. Gonzalo, M. Montero, G. Obied, and C. Vafa, Dark dimension gravitons as dark matter, J. High Energy Phys. 11 (2023) 109.
[26] L. A. Anchordoqui, I. Antoniadis, and D. Lüst, Aspects of the dark dimension in cosmology, Phys. Rev. D **107**, 083530 (2023).
[27] L. A. Anchordoqui, I. Antoniadis, N. Cribiori, D. Lüst, and M. Scalisi, The scale of supersymmetry breaking and the dark dimension, J. High Energy Phys. 05 (2023) 060.
[28] D. van de Heisteeg, C. Vafa, M. Wiesner, and D. H. Wu, Bounds on field range for slowly varying positive potentials, J. High Energy Phys. 02 (2024) 175.
[29] N. T. Noble, J. F. Soriano, and L. A. Anchordoqui, Probing the dark dimension with Auger data, Phys. Dark Universe **42**, 101278 (2023).
[30] L. A. Anchordoqui, I. Antoniadis, and J. Cunat, The dark dimension and the Standard Model landscape, Phys. Rev. D **109**, 016028 (2024).
[31] A. Makridou, Swampland program: Cobordism, tadpoles, and the dark dimension, 10.5282/edoc.32315 (2023).
[32] J. A. P. Law-Smith, G. Obied, A. Prabhu, and C. Vafa, Astrophysical constraints on decaying dark gravitons, arXiv:2307.11048.
[33] L. A. Anchordoqui, I. Antoniadis, K. Benakli, J. Cunat, and D. Lüst, Searching for neutrino-modulino oscillations

at the forward physics facility, Phys. Lett. B **850**, 138530 (2024).
[34] L. A. Anchordoqui, I. Antoniadis, and D. Lüst, Fuzzy dark matter and the dark dimension, Eur. Phys. J. C **84**, 273 (2024).
[35] L. A. Anchordoqui and I. Antoniadis, Large extra dimensions from higher-dimensional inflation, Phys. Rev. D **109**, 103508 (2024).
[36] G. Obied, C. Dvorkin, E. Gonzalo, and C. Vafa, Dark dimension and decaying dark matter gravitons, Phys. Rev. D **109**, 063540 (2024).
[37] L. A. Anchordoqui, I. Antoniadis, and D. Lüst, Anti-de Sitter → de Sitter transition driven by Casimir forces and mitigating tensions in cosmological parameters, arXiv:2312.12352.
[38] L. A. Anchordoqui, I. Antoniadis, and D. Lüst, The dark dimension, the swampland, and the dark matter fraction composed of primordial near-extremal black holes, Phys. Rev. D **109**, 095008 (2024).
[39] C. Vafa, Swamplandish unification of the dark sector, arXiv:2402.00981.
[40] K. R. Dienes and B. Thomas, Dynamical dark matter I: Theoretical overview, Phys. Rev. D **85**, 083523 (2012).
[41] G. Dvali, A microscopic model of holography: Survival by the burden of memory, arXiv:1810.02336.
[42] G. Dvali, L. Eisemann, M. Michel, and S. Zell, Black hole metamorphosis and stabilization by memory burden, Phys. Rev. D **102**, 103523 (2020).
[43] A. Alexandre, G. Dvali, and E. Koutsangelas, New mass window for primordial black holes as dark matter from memory burden effect, arXiv:2402.14069.
[44] J. H. Schwarz, Comments concerning a hypothetical mesoscopic dark dimension, arXiv:2403.12899.
[45] S. W. Hawking, Black hole explosions, Nature (London) **248**, 30 (1974).
[46] S. W. Hawking, Particle creation by black holes, Commun. Math. Phys. **43**, 199 (1975); **46**, 206(E) (1976).
[47] S. A. Fulling, Nonuniqueness of canonical field quantization in Riemannian space-time, Phys. Rev. D **7**, 2850 (1973).
[48] P. C. W. Davies, Scalar particle production in Schwarzschild and Rindler metrics, J. Phys. A **8**, 609 (1975).
[49] W. G. Unruh, Notes on black hole evaporation, Phys. Rev. D **14**, 870 (1976).
[50] W. Rindler, Kruskal space and the uniformly accelerated frame, Am. J. Phys. **34**, 1174 (1966).
[51] S. W. Hawking, Black holes and thermodynamics, Phys. Rev. D **13**, 191 (1976).
[52] G. F. Giudice, R. Rattazzi, and J. D. Wells, Quantum gravity and extra dimensions at high-energy colliders, Nucl. Phys. **B544**, 3 (1999).
[53] F. R. Tangherlini, Schwarzschild field in *n* dimensions and the dimensionality of space problem, Nuovo Cimento **27**, 636 (1963).
[54] R. C. Myers and M. J. Perry, Black holes in higher dimensional space-times, Ann. Phys. (N.Y.) **172**, 304 (1986).
[55] P. C. Argyres, S. Dimopoulos, and J. March-Russell, Black holes and submillimeter dimensions, Phys. Lett. B **441**, 96 (1998).
[56] L. A. Anchordoqui, J. L. Feng, H. Goldberg, and A. D. Shapere, Black holes from cosmic rays: Probes of extra dimensions and new limits on TeV scale gravity, Phys. Rev. D **65**, 124027 (2002).
[57] L. Parker, Probability distribution of particles created by a black hole, Phys. Rev. D **12**, 1519 (1975).
[58] R. M. Wald, On particle creation by black holes, Commun. Math. Phys. **45**, 9 (1975).
[59] S. W. Hawking, Breakdown of predictability in gravitational collapse, Phys. Rev. D **14**, 2460 (1976).
[60] D. N. Page, Particle emission rates from a black hole: Massless particles from an uncharged, nonrotating hole, Phys. Rev. D **13**, 198 (1976).
[61] D. N. Page, Particle emission rates from a black hole II: Massless particles from a rotating hole, Phys. Rev. D **14**, 3260 (1976).
[62] D. N. Page, Particle emission rates from a black hole III: Charged leptons from a nonrotating hole, Phys. Rev. D **16**, 2402 (1977).
[63] P. Kanti and J. March-Russell, Calculable corrections to brane black hole decay I: The scalar case, Phys. Rev. D **66**, 024023 (2002).
[64] A. Ireland, S. Profumo, and J. Scharnhorst, Gravitational waves from primordial black hole evaporation with large extra dimensions, arXiv:2312.08508.
[65] R. Emparan, G. T. Horowitz, and R. C. Myers, Black holes radiate mainly on the brane, Phys. Rev. Lett. **85**, 499 (2000).
[66] S. Dimopoulos and G. L. Landsberg, Black holes at the LHC, Phys. Rev. Lett. **87**, 161602 (2001).
[67] T. Han, G. D. Kribs, and B. McElrath, Black hole evaporation with separated fermions, Phys. Rev. Lett. **90**, 031601 (2003).
[68] L. Anchordoqui and H. Goldberg, Black hole chromosphere at the CERN LHC, Phys. Rev. D **67**, 064010 (2003).
[69] A. Chamblin, R. Emparan, C. V. Johnson, and R. C. Myers, Charged AdS black holes and catastrophic holography, Phys. Rev. D **60**, 064018 (1999).
[70] N. Cribiori, M. Dierigl, A. Gnecchi, D. Lüst, and M. Scalisi, Large and small non-extremal black holes, thermodynamic dualities, and the swampland, J. High Energy Phys. 10 (2022) 093.
[71] I. Basile, N. Cribiori, D. Lüst, and C. Montella, Minimal black holes and species thermodynamics, arXiv:2401.06851.
[72] D. N. Page, Information in black hole radiation, Phys. Rev. Lett. **71**, 3743 (1993).
[73] D. N. Page, Time dependence of Hawking radiation entropy, J. Cosmol. Astropart. Phys. 09 (2013) 028.
[74] G. Dvali, F. Kühnel, and M. Zantedeschi, Primordial black holes from confinement, Phys. Rev. D **104**, 123507 (2021).
[75] S. Ryu and T. Takayanagi, Holographic derivation of entanglement entropy from AdS/CFT, Phys. Rev. Lett. **96**, 181602 (2006).
[76] V. E. Hubeny, M. Rangamani, and T. Takayanagi, A covariant holographic entanglement entropy proposal, J. High Energy Phys. 07 (2007) 062.
[77] A. Lewkowycz and J. Maldacena, Generalized gravitational entropy, J. High Energy Phys. 08 (2013) 090.

[78] G. Penington, Entanglement wedge reconstruction and the information paradox, J. High Energy Phys. 09 (2020) 002.
[79] A. Almheiri, N. Engelhardt, D. Marolf, and H. Maxfield, The entropy of bulk quantum fields and the entanglement wedge of an evaporating black hole, J. High Energy Phys. 12 (2019) 063.
[80] A. Almheiri, R. Mahajan, J. Maldacena, and Y. Zhao, The Page curve of Hawking radiation from semiclassical geometry, J. High Energy Phys. 03 (2020) 149.
[81] G. Penington, S. H. Shenker, D. Stanford, and Z. Yang, Replica wormholes and the black hole interior, J. High Energy Phys. 03 (2022) 205.
[82] A. Almheiri, T. Hartman, J. Maldacena, E. Shaghoulian, and A. Tajdini, Replica wormholes and the entropy of Hawking radiation, J. High Energy Phys. 05 (2020) 013.
[83] K. Hashimoto, N. Iizuka, and Y. Matsuo, Islands in Schwarzschild black holes, J. High Energy Phys. 06 (2020) 085.
[84] H. Z. Chen, Z. Fisher, J. Hernandez, R. C. Myers, and S. M. Ruan, Evaporating black holes coupled to a thermal bath, J. High Energy Phys. 01 (2021) 065.
[85] R. Bousso and G. Penington, Islands far outside the horizon, arXiv:2312.03078.
[86] Y. B. Zel'dovich and I. D. Novikov, The hypothesis of cores retarded during expansion and the hot cosmological model, Sov. Astron. AJ (Engl. Transl.), **10**, 602 (1967).
[87] S. Hawking, Gravitationally collapsed objects of very low mass, Mon. Not. R. Astron. Soc. **152**, 75 (1971).
[88] B. J. Carr and S. W. Hawking, Black holes in the early Universe, Mon. Not. R. Astron. Soc. **168**, 399 (1974).
[89] B. J. Carr, The primordial black hole mass spectrum, Astrophys. J. **201**, 1 (1975).
[90] B. Carr and F. Kuhnel, Primordial black holes as dark matter: Recent developments, Annu. Rev. Nucl. Part. Sci. **70**, 355 (2020).
[91] A. M. Green and B. J. Kavanagh, Primordial black holes as a dark matter candidate, J. Phys. G **48**, 043001 (2021).
[92] P. Villanueva-Domingo, O. Mena, and S. Palomares-Ruiz, A brief review on primordial black holes as dark matter, Front. Astron. Space Sci. **8**, 87 (2021).
[93] E. Bagui *et al.* (LISA Cosmology Working Group), Primordial black holes and their gravitational-wave signatures, arXiv:2310.19857.
[94] B. J. Carr, K. Kohri, Y. Sendouda, and J. Yokoyama, New cosmological constraints on primordial black holes, Phys. Rev. D **81**, 104019 (2010).
[95] S. Clark, B. Dutta, Y. Gao, L. E. Strigari, and S. Watson, Planck constraint on relic primordial black holes, Phys. Rev. D **95**, 083006 (2017).
[96] W. DeRocco and P. W. Graham, Constraining primordial black hole abundance with the Galactic 511 keV line, Phys. Rev. Lett. **123**, 251102 (2019).
[97] R. Laha, Primordial black holes as a dark matter candidate are severely constrained by the Galactic Center 511 keV γ-ray line, Phys. Rev. Lett. **123**, 251101 (2019).
[98] B. Dasgupta, R. Laha, and A. Ray, Neutrino and positron constraints on spinning primordial black hole dark matter, Phys. Rev. Lett. **125**, 101101 (2020).
[99] C. Keith and D. Hooper, 511 keV excess and primordial black holes, Phys. Rev. D **104**, 063033 (2021).
[100] S. Mittal, A. Ray, G. Kulkarni, and B. Dasgupta, Constraining primordial black holes as dark matter using the global 21-cm signal with x-ray heating and excess radio background, J. Cosmol. Astropart. Phys. 03 (2022) 030.
[101] R. Laha, J. B. Muñoz, and T. R. Slatyer, INTEGRAL constraints on primordial black holes and particle dark matter, Phys. Rev. D **101**, 123514 (2020).
[102] J. Berteaud, F. Calore, J. Iguaz, P. D. Serpico, and T. Siegert, Strong constraints on primordial black hole dark matter from 16 years of INTEGRAL/SPI observations, Phys. Rev. D **106**, 023030 (2022).
[103] M. Korwar and S. Profumo, Updated constraints on primordial black hole evaporation, J. Cosmol. Astropart. Phys. 05 (2023) 054.
[104] R. A. Allsman *et al.* (MACHO Collaboration), MACHO project limits on black hole dark matter in the 1–30 solar mass range, Astrophys. J. Lett. **550**, L169 (2001).
[105] P. Tisserand *et al.* (EROS-2 Collaboration), Limits on the MACHO content of the Galactic Halo from the EROS-2 survey of the Magellanic clouds, Astron. Astrophys. **469**, 387 (2007).
[106] K. Griest, A. M. Cieplak, and M. J. Lehner, Experimental limits on primordial black hole dark matter from the first 2 yr of Kepler data, Astrophys. J. **786**, 158 (2014).
[107] M. Oguri, J. M. Diego, N. Kaiser, P. L. Kelly, and T. Broadhurst, Understanding caustic crossings in giant arcs: Characteristic scales, event rates, and constraints on compact dark matter, Phys. Rev. D **97**, 023518 (2018).
[108] H. Niikura, M. Takada, S. Yokoyama, T. Sumi, and S. Masaki, Constraints on Earth-mass primordial black holes from OGLE 5-year microlensing events, Phys. Rev. D **99**, 083503 (2019).
[109] D. Croon, D. McKeen, N. Raj, and Z. Wang, Subaru-HSC through a different lens: Microlensing by extended dark matter structures, Phys. Rev. D **102**, 083021 (2020).
[110] A. Gould, Femtolensing of gamma-ray bursters, Astrophys. J. Lett. **386**, L5 (1992).
[111] A. Barnacka, J. F. Glicenstein, and R. Moderski, New constraints on primordial black holes abundance from femtolensing of gamma-ray bursts, Phys. Rev. D **86**, 043001 (2012).
[112] A. Katz, J. Kopp, S. Sibiryakov, and W. Xue, Femtolensing by dark matter revisited, J. Cosmol. Astropart. Phys. 12 (2018) 005.
[113] J. F. Navarro, C. S. Frenk, and S. D. M. White, The structure of cold dark matter halos, Astrophys. J. **462**, 563 (1996).
[114] J. A. de Freitas Pacheco, E. Kiritsis, M. Lucca, and J. Silk, Quasiextremal primordial black holes are a viable dark matter candidate, Phys. Rev. D **107**, 123525 (2023).
[115] V. Thoss, A. Burkert, and K. Kohri, Breakdown of Hawking evaporation opens new mass window for primordial black holes as dark matter candidate, arXiv:2402.17823.
[116] K. R. Dienes, E. Dudas, and T. Gherghetta, Neutrino oscillations without neutrino masses or heavy mass scales:

A higher dimensional seesaw mechanism, Nucl. Phys. **B557**, 25 (1999).
[117] N. Arkani-Hamed, S. Dimopoulos, G. R. Dvali, and J. March-Russell, Neutrino masses from large extra dimensions, Phys. Rev. D **65**, 024032 (2001).
[118] G. R. Dvali and A. Y. Smirnov, Probing large extra dimensions with neutrinos, Nucl. Phys. B **B563**, 63 (1999).
[119] A. Chamblin, S. W. Hawking, and H. S. Reall, Brane world black holes, Phys. Rev. D **61**, 065007 (2000).
[120] L. A. Anchordoqui, H. Goldberg, and A. D. Shapere, Phenomenology of Randall-Sundrum black holes, Phys. Rev. D **66**, 024033 (2002).
[121] A. Bedroya, C. Vafa, and D. H. Wu, The tale of three scales: The Planck, the species, and the black hole scales, arXiv:2403.18005.